J. Plasma Fusion Res. SERIES, Vol. 2 (1999) 423–426

Growth of Laser Ripple in a Collisional Magnetoplasma and Its Effect on Plasma Wave Excitation

SINGH Nareshpal and SINGH Tarsem

Department of Physics, Guru Nanak Dev University, Amritsar-143005, India

(Received: 7 December 1998 / Accepted: 22 July 1999)

Abstract

Growth of a radially symmetrical ripple, superimposed on a Gaussian laser beam in collisional magnetoplasma is investigated. The effect of the magnetic field and the intensity of the laser on the growth of ripple is presented. Furthermore, the effect of the growing ripple on the excitation of an electron plasma wave has also been studied. The combined effect of increased intensity and magnetic field is observed to suppress the growth of ripple as well as the excitation of the plasma wave.

Keywords:

ICF, self-focusing, EPW, ripple, Gaussian

1. Introduction

The nonlinear interactions of intense laser beams have assumed importance on account of their relevance to controlled thermonuclear fusion [1]. In inertial confinement fusion (ICF), the important problem is the efficient coupling of the laser beam to plasma. This coupling is usually nonlinear in nature and parametric processes which are excited, do not occur in isolation [2]. In order to understand the physics of the laser fusion experiments, it is important to investigate the interdependance of these processes. Some processes are modelled by considering the ripple model [3]. The nonlinearity considered here is of collisional type, which ensues from temperature dependent collision frequency.

2. Nonlinear Dielectric Tensor

Consider the propagation of a laser beam of angular frequency ω_0 in a homogeneous magnetoplasma along the static magnetic field B_0 coincident with z-axis. The main beam has a Gaussian intensity distribution along the wavefront . In linear approximation, one can assume laser to be propagating in either of the two modes of propagation, viz. ordinary and extraordinary. In the presence of Gaussian ripple [3], the total electric vector can be written as

$$\boldsymbol{E}_{t\pm} = \boldsymbol{E}_{0\pm} \exp\left[\iota(\omega_0 t - k_{0\pm} z)\right] + \boldsymbol{E}_{1\pm} \exp\left[\iota(\omega_0 t - k_{0\pm} z)\right]. \quad (1)$$

Here $\boldsymbol{E}_{0\pm}$ and $\boldsymbol{E}_{1\pm}$ are the electric vectors of the main beam and the ripple and their initial intensity distributions are given as

$$\boldsymbol{E}_{0\pm} \cdot \boldsymbol{E}^*_{0\pm} = E_{00}^2 \exp\left(\frac{-r^2}{r_0^2}\right),$$

$$\boldsymbol{E}_{1\pm} \cdot \boldsymbol{E}^*_{1\pm} = E_{00}^2 \left(\frac{r}{r_{10}}\right)^{2n} \exp\left(-\frac{r^2}{r_{10}^2}\right),$$

where n is a positive number and r_{10} is the width of the ripple. As n increases, the maximum $r_{\max} = r_{10}\sqrt{n}$ of the ripple shifts away from the axis. In the presence of rippled beam, the modified electron concentration may be written as

Corresponding author's e-mail: nssaini@excite.com

$$N_{0e}=N_0\left[1-\frac{8}{3}\alpha_0 M/m\frac{\boldsymbol{E}_{t\pm}\cdot\boldsymbol{E}^*_{t\pm}}{(1-\frac{\omega_c}{\omega_0})^2}\frac{1}{\left(2+\frac{8}{3}\alpha_0 M/m\frac{\boldsymbol{E}_{t\pm}\cdot\boldsymbol{E}^*_{t\pm}}{(1-\frac{\omega_c}{\omega_0})^2}\right)}\right], \quad (2)$$

where symbols have their usual meanings [4].

3. Solution of the Wave Equation

The total electric vector $\boldsymbol{E}_{t\pm}$ in WKB approximation satisfies the wave equation

$$\frac{\partial^2 \boldsymbol{E}_{t\pm}}{\partial z^2}+\frac{1}{2}\left(1+\frac{\varepsilon_{0\pm}}{\varepsilon_{0zz}}\right)\left(\frac{\partial^2}{\partial x^2}+\frac{\partial^2}{\partial y^2}\right)\boldsymbol{E}_{t\pm}+\frac{\omega_0^2}{c^2}\varepsilon_{\pm}\boldsymbol{E}_{t\pm}=0. \quad (3)$$

Therefore, the electric vectors of the main beam $\boldsymbol{E}_{0\pm}$ and the ripple $\boldsymbol{E}_{1\pm}$ satisfy the following equations:

$$\frac{\partial^2 \boldsymbol{E}_{0+}}{\partial z^2}+\frac{1}{2}\left(1+\frac{\varepsilon_{0\pm}}{\varepsilon_{0zz}}\right)\left(\frac{\partial^2}{\partial x^2}+\frac{\partial^2}{\partial y^2}\right)\boldsymbol{E}_{0\pm}+\frac{\omega_0^2}{c^2}\left[\varepsilon_{0\pm}+\Phi_+(\boldsymbol{E}_{0+}\cdot\boldsymbol{E}^*_{0+})\right]\boldsymbol{E}_{0+}=0, \quad (4)$$

$$\frac{\partial^2 \boldsymbol{E}_{1+}}{\partial z^2}+\frac{1}{2}\left(1+\frac{\varepsilon_{0\pm}}{\varepsilon_{0zz}}\right)\left(\frac{\partial^2}{\partial x^2}+\frac{\partial^2}{\partial y^2}\right)\boldsymbol{E}_{1+}+\frac{\omega_0^2}{c^2}\left[\varepsilon_{0+}+\Phi_+(\boldsymbol{E}_{t+}\cdot\boldsymbol{E}^*_{t+})\right]\boldsymbol{E}_{1+}+\frac{\omega_0^2}{c^2}\left[\Phi_+(\boldsymbol{E}_{t+}\cdot\boldsymbol{E}^*_{t+})-\Phi_+(\boldsymbol{E}_{0+}\cdot\boldsymbol{E}^*_{0+})\right]\boldsymbol{E}_{0+}=0. \quad (5)$$

For the sake of simplicity only one mode has been chosen, although analysis is valid for the other mode as well. Following Akhmanov *et al.* [5] and Singh *et al.* [3], the equations (4) and (5) are solved using paraxial ray approximation (PRA) and the dimensionless beam width parameters of main beam f_{0+} and ripple f_1 are governed by the following equations:

$$\frac{d^2 f_{0+}}{dz^2}=\frac{\left(1+\frac{\varepsilon_{0\pm}}{\varepsilon_{0zz}}\right)^2}{4k_{0+}^2 r_0^4 f_{0+}^3}-\frac{\left(1+\frac{\varepsilon_{0\pm}}{\varepsilon_{0zz}}\right)}{2\varepsilon_{0+} r_0^2 f_{0+}^2\left(1-\frac{\omega_c}{\omega_0}\right)^3}\alpha E_{00}^2\frac{\omega_p^2}{\omega_0^2}\left[\frac{1}{2+\frac{\alpha E_{00}^2}{(1-\frac{\omega_c}{\omega_0})^2 f_{0+}^2}}-\frac{\alpha E_{00}^2}{f_{0+}^2(1-\frac{\omega_c}{\omega_0})^2\left(2+\frac{\alpha E_{00}^2}{(1-\frac{\omega_c}{\omega_0})^2 f_{0+}^2}\right)^2}\right], \quad (6)$$

$$\frac{d^2 f_1}{dz^2}=\frac{c^2\left(1+\frac{\varepsilon_{0\pm}}{\varepsilon_{0zz}}\right)^2}{4\omega_0^2 r_{10}^4 f_1\varepsilon_{0+}}-\frac{\left(1+\frac{\varepsilon_{0\pm}}{\varepsilon_{0zz}}\right)f_1\alpha E_{00}^2\omega_p^2}{2\varepsilon_{0+}\omega_0^2 r_0^2(1-\frac{\omega_c}{\omega_0})^3}\left[\frac{T_2}{(2+\frac{\alpha E_{00}^2 T_3}{(1-\frac{\omega_c}{\omega_0})^2})}\left(1-\frac{\alpha E_{00}^2 T_3}{(1-\frac{\omega_c}{\omega_0})^2[2+\frac{\alpha E_{00}^2 T_3}{(1-\frac{\omega_c}{\omega_0})^2}]}\right)+\frac{2\cos^2\phi_p T_4}{f_0^4}\left(\frac{(2+2\alpha E_{00}^2 T_4)}{[2+\frac{\alpha E_{00}^2 T_4}{f_0^2(1-\frac{\omega_c}{\omega_0})^2}]^2}-\frac{2(\alpha E_{00}^2)^2 T_4^2}{(1-\frac{\omega_c}{\omega_0})^2 f_0^4[2+\frac{\alpha E_{00}^2 T_4}{f_0^2(1-\frac{\omega_c}{\omega_0})^2}]^3}\right)\right], \quad (7)$$

$$T_2=\frac{\exp(-\frac{r_{10}^2 f_1^2 n}{r_0^2 f_0^2})}{f_0^4}+\frac{\cos\phi_p n^{n/2}(E_{100}/E_{00})}{f_0^3 f_1}\exp(-\int_0^z k_i\,dz)\exp(-\frac{n}{2}-\frac{r_{10}^2 f_1^2 n}{2r_0^2 f_0^2}),$$

$$T_3=\frac{\exp(-\frac{r_{10}^2 f_1^2 n}{r_0^2 f_0^2})}{f_0^2}+\frac{2\cos\phi_p n^{n/2}(E_{100}/E_{00})}{f_0 f_1}\exp(-\frac{n}{2}-\frac{r_{10}^2 f_1^2 n}{2r_0^2 f_0^2}),$$

$$T_4=\exp(-\frac{r_{10}^2 f_1^2 n}{r_0^2 f_0^2}),$$

where $\alpha=\frac{8M}{3m}\alpha_0$ The initial conditions on f_{0+} and f_1, for a plane wavefront, are $\frac{df_{0+}}{dz}=0=\frac{df_1}{dz}$ and $f_{0+}=1.0=f_1$ at $z=0$. The expression for the growth rate of ripple can be written as

$$k_i\simeq\frac{1}{2}\frac{\omega_0^2}{c^2}\frac{1}{k_0}\frac{\omega_p^2}{\omega_0^2}\frac{\alpha A_0^2}{(1-\frac{\omega_c}{\omega_0})^3}\sin(2\phi_p)\left[\frac{1}{2+\frac{\alpha\boldsymbol{E}_{0\pm}\cdot\boldsymbol{E}^*_{0\pm}}{(1-\frac{\omega_c}{\omega_0})^2}}-\frac{\alpha\boldsymbol{E}_{0\pm}\cdot\boldsymbol{E}^*_{0\pm}}{(1-\frac{\omega_c}{\omega_0})^2}\frac{1}{\left[2+\frac{\alpha\boldsymbol{E}_{0\pm}\cdot\boldsymbol{E}^*_{0\pm}}{(1-\frac{\omega_c}{\omega_0})^2}\right]^2}\right]. \quad (8)$$

It is interesting to note that if the main beam has a uniform intensity distribution along the wavefront ($r_0\to\infty$ and $f_{0+}=1$) and $\omega_c=0$, then the growth rate is comparable to the growth rate of the filamentation instability.

4. Excitation of Electron Plasma Wave

A weak electron plasma wave (EPW) is nonlinearly coupled to rippled laser beam via modified background density. Thus, self-focusing of main beam and dynamics of growth of ripple affect the excitation of plasma wave substantially. The excitation process is governed by the following equations:

$$\frac{\partial N_e}{\partial t} + \nabla \cdot (N_e \boldsymbol{V}) = 0, \; \boldsymbol{m}\frac{\partial \boldsymbol{V}}{\partial t} = -e\boldsymbol{E}_t - \frac{e\boldsymbol{V} \times \boldsymbol{B}}{c} - \frac{\gamma}{N_e} \nabla \boldsymbol{P}_e, \quad (9)$$

supplemented by Poissons equation, $\nabla \cdot \boldsymbol{E}' = -4\pi e n'$. Here $\boldsymbol{V}$ is the electron drift velocity, N_e is the total electron density, $\boldsymbol{B}$ is the external magnetic field, $\boldsymbol{E}_t$ is the total electric field in the plasma. $\boldsymbol{E}'$ is the longitudnal part of the electric field and n' are the corresponding density perturbations. In perturbation analysis we can write

$$N_e = N_{0e} + n', \quad \boldsymbol{V} = \boldsymbol{V}_0 + \boldsymbol{V}', \quad \boldsymbol{E}_t = \boldsymbol{E} + \boldsymbol{E}', \quad (10)$$

where $n' \ll N_{0e}$, $V' \ll V_0$, $E' \ll E$. Using these approximations and following [6], we obtain the following equation for the excitation of EPW in first order approximation.

$$\frac{d^2 n'}{dt^2} - v_{th}^2 \nabla^2 n' + \omega_p^2 \frac{N_{0e}}{N_0} n' = 0, \quad (11)$$

where $v_{th}^2 = \gamma k_B T_e / m$. Equation (11) is electron plasma wave coupled to main laser beam and ripple through modified background density N_{0e}. Thus, in case pump and ripple change the background density due to focusing/defocusing, the characterstics of EPW are correspondingly modified. Equation (11) is solved following Sodha *et al.* [7] and the dimensionless beam width parameter f_p for EPW is governed by the following equation:

$$\frac{d^2 f_p}{dz^2} = \frac{1}{k^2 a_0^4 f_p^3} - \frac{\omega_p^2}{k^2 v_{th}^2} f_p \left(\frac{2\alpha}{(1-\frac{\omega_c}{\omega_0})^2 (2 + \frac{\alpha}{(1-\frac{\omega_c}{\omega_0})^2} \boldsymbol{E}_t \cdot \boldsymbol{E}_t^*)^2} \right) \left(\frac{E_{00} E_{100}}{f_0 f_1} \cos(\phi_p) n^{n/2} \exp(-\int_0^z k_i dz) \frac{1}{r_0^2 f_0^2} \exp\left(-\frac{n}{2} - \frac{r_{10}^2 f_1^2 n}{r_0^2 f_0^2} \right) + \frac{E_{00}^2}{r_0^2 f_0^4} \exp[-\frac{r_{10}^2 f_1^2 n}{r_0^2 f_0^2}] \right). \quad (12)$$

5. Discussion

It is due to coupling of ripple with main beam equations (6) and (7), the ripple is expected to grow/decay in the plasma. The growth rate of the ripple k_i, given by eq.(8), depends on externally applied magnetic field, pump and plasma parameters and on the distance of propagation. Analytical solution of equations (6), (7) and (12) is not possible. We, therefore, seek numerical solution of these equations for the following set of parameters: $(r_0 \omega_p / c)^2 = 20.0$, $\omega_p / \omega_0 = 0.5$, $\omega_0 = 1.778 \times 10^{14}$ rad/s, $n = 2.0$, $2\phi_p = \pi/2$, $r_{10}^2 / r_2^0 = 0.3$, $r_{10}/a_0 = 0.7$, $\alpha E_{00}^2 = 5.0$, $\omega_c / \omega_0 = 0.2$.

In laser fusion experiments, beams with nonuniform intensity such as considered here, have an index of refraction dependent on local field intensity and can produce its own dielectric waveguide. Small scale intensity spike/ripple on such a beam can grow unstably by the same self-focusing mechanism and its growth rate is comparable to filamentation intensity [7]. The ripple, which is coupled to the main beam, grows at the cost of the main beam and results in filamentary break. Its dynamics with the distance of propagation is crucial to physical insight of underdense plasma and is one of the key issues of laser induced fusion. The growth dynamics has deleterious effect as it affects the absorption process as well as spoils the symmetry of implosion due to hydrodynamics instabilities. Furthermore, as magnetic fields, external or self-generated, are usually present in laser plasma experiments, this necessitates the investigation of observing the effect of magnetic field on the intensity dynamics of ripple. Figure 1 and Fig. 2 display the variation of the normalized axial intensity of the laser ripple against dimensionless distance of propagation ξ ($= zc/\omega_0 r_{10}^2$) for different values of magnetic fields and intensities. It is observed that effect of increasing magnetic field and intensity is to suppress the growth of ripple k_i. Such a case is favourable to the laser fusion.

Excitation of EPW, used in laser heating expriments is governed by eq.(11), where the last term represents the coupling of EPW to the modified background. Figure 3 and Fig. 4 depict the variation of the plasma density perturbation associated with EPW vs. ξ. It is observed that the effect of increase of magnetic field and intensity is again to suppress the density perturbation. This is due to the fact that transport of carriers density contributing to EPW is inhibited by the magnetic field. Thus, we conclude that although the effect of increased intensity of the laser beam and magnetic field is useful in suppressing the growth of

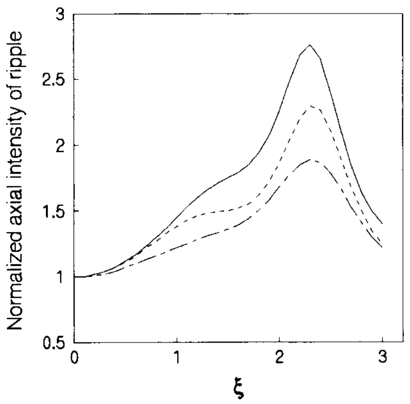

Fig. 1 Normalized axial intensity of the ripple plotted against the normalized distance of propagation ξ (= $zc/\omega_0 r_{10}^2$) in a collisional magnetoplasma for the following set of parameters: $(\frac{r_0\omega_p}{c})^2 = 20.0$, $\frac{\omega_p}{\omega_0} = 0.5$, $\omega_0 = 1.778 \times 10^{14}$ rad/s, $n = 2.0$, $2\pi_p = \frac{\pi}{2}$, $\frac{r_{10}^2}{r_0^2} = 0.3$, $\frac{r_{10}}{a_0} = 0.7$, $\alpha E_{00}^2 = 5.0$, $\frac{\omega_c}{\omega_0} = 0.2$. The solid curve is for zero field, dotted and semidotted for $\frac{\omega_c}{\omega_0} = 0.4$ and $\frac{\omega_c}{\omega_0} = 0.6$.

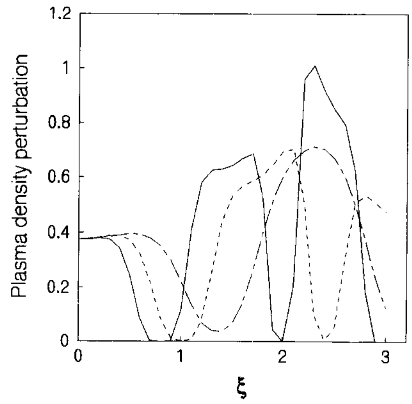

Fig. 3 Plasma density perturbation associated with the excited electron plasma wave vs the normalized distance of propagation ξ in the collisional magnetoplasma for the parameters mentioned in Fig. caption 1. The solid curve is for zero field whereas dotted and semidotted are for $\frac{\omega_c}{\omega_0} = 0.4$ and $\frac{\omega_c}{\omega_0} = 0.6$.

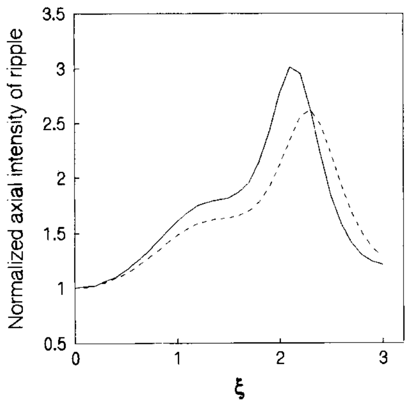

Fig. 2 Normalized axial intensity of the ripple plotted against the normalized distance of propagation ξ (= $zc/\omega_0 r_{10}^2$) in a collisional magnetoplasma for the same parameters as mentioned in Fig. caption 1. The solid curve is for $\alpha E_{00}^2 = 4.0$ and dotted curve is for $\alpha E_{00}^2 = 5.0$.

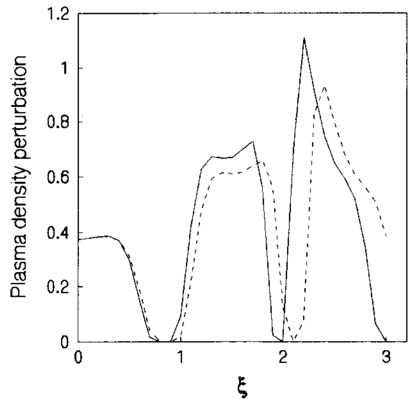

Fig. 4 Plasma density perturbation associated with the excited electron plasma wave vs the normalized distance of propagation ξ in the collisional magnetoplasma for the parameters mentioned in Fig. caption 1. The solid curve is for $\alpha E_{00}^2 = 4.0$ and dotted curve is for $\alpha E_{00}^2 = 5.0$.

ripple, but it also suppresses the excitation of the plamsa wave. This counteracts the heating scheme, in which the excited EPW dumps its energy to plasma due to wave-particle interaction.

References

[1] S.C. Abbi and H. Mahr, Phy. Rev. Lett. **26**, 604 (1971).

[2] R.D. Jones *et al.*, Phys. Fluids **31**, 1249 (1988).

[3] A. Singh and T. Singh, IL Nuovo Cimento 'D' **3**, 363 (1991).

[4] M.S. Sodha, V.K. Tripathi and A.K. Ghatak, Prog. Optics **13**, 171 (1976).

[5] S.A. Akhmanov *et al.*, Sov. Phys. Usp. **10**, 609 (1968).

[6] T. Singh and M. Salimullah, IL Nuovo Cimento 'D' **9**, 987 (1987).

[7] M.S. Sodha, T. Singh, D.P. Singh and R.P. Sharma, Phys. Fluids **24**, 914 (1981).